High Precision Deformation Monitoring at the Geodynamic Observatory Moxa/Thuringia, Germany

The Three-Component Strainmeter Assembly

Peter Schindler, Thomas Jahr, Gerhard Jentzsch, and Nina Kukowski

Abstract

With strainmeters the observation of crustal deformation is possible with a resolution better than 10^{-9} m. At the Geodynamic Observatory Moxa in Thuringia/Germany an assembly of strainmeters of different types is recording deformation. Deformation mainly results from the tidal forces of sun and moon acting on the Earth, but also comes from seismic wave propagation or regional and local sources.

Here we describe the results of an analysis of five time-series, each spanning 482 days, obtained from the different instruments and areal strain. We focus on the Earth tides but also look on the resonance of the Earth's core to tidal forcing, the Nearly Diurnal Free Wobble. Even if not all five time-series show the resonance, its finding, especially in strain data, confirms the high data quality and sensitivity of the instruments.

The analysis of the strainmeter data shows the comparability of the data from the different instruments as well as the good data quality connected to the very low noise level at the Geodynamic Observatory Moxa. Comparison with ocean loading shows that strong effects from local conditions like topography or rock inhomogeneities exist.

Keywords

Earth tides • Strainmeter systems • Deformation monitoring • Nearly Diurnal Free Wobble

PACS 91.10.Kg · 91.10.Tq

1 Introduction

Strainmeters allow to observe deformation with a high resolution better than 10^{-9} m. Since 1964, at the Geodynamic Observatory Moxa in Thuringia/Germany two quartz tube strainmeters have continuously been observing deformation. In 2002, a laser strainmeter, and in 2005 a borehole strainmeter were installed (Jahr et al. 2006). This arrangement enables observation of load-induced deformation effects of barometric pressure fields moving over the observatory and the measurement of hydrologically induced signals as well as the study of low-frequency signals like the Earth tides and the free modes of the Earth.

2 Installation and Data Acquisition

The Geodynamic Observatory Moxa (Fig. 1) consists of a three-part building located at the foot of a hill, and a gallery dug horizontally into the adjacent slope. The gallery is separated from the building by several doors to keep environmental conditions, especially temperature, as stable as possible. Its instrumentation consists of different types of measurement systems, including besides strainmeters also tiltmeters, seismometers, a superconducting gravimeter as

P. Schindler (✉) • T. Jahr • G. Jentzsch • N. Kukowski
Friedrich Schiller University Jena, Institute of Geosciences, Burgweg 11, 07749 Jena, Germany
e-mail: peter.schindler@uni-jena.de

(G. Jentzsch now retired)

C. Rizos and P. Willis (eds.), *Earth on the Edge: Science for a Sustainable Planet*, International Association of Geodesy Symposia 139, DOI 10.1007/978-3-642-37222-3_18,

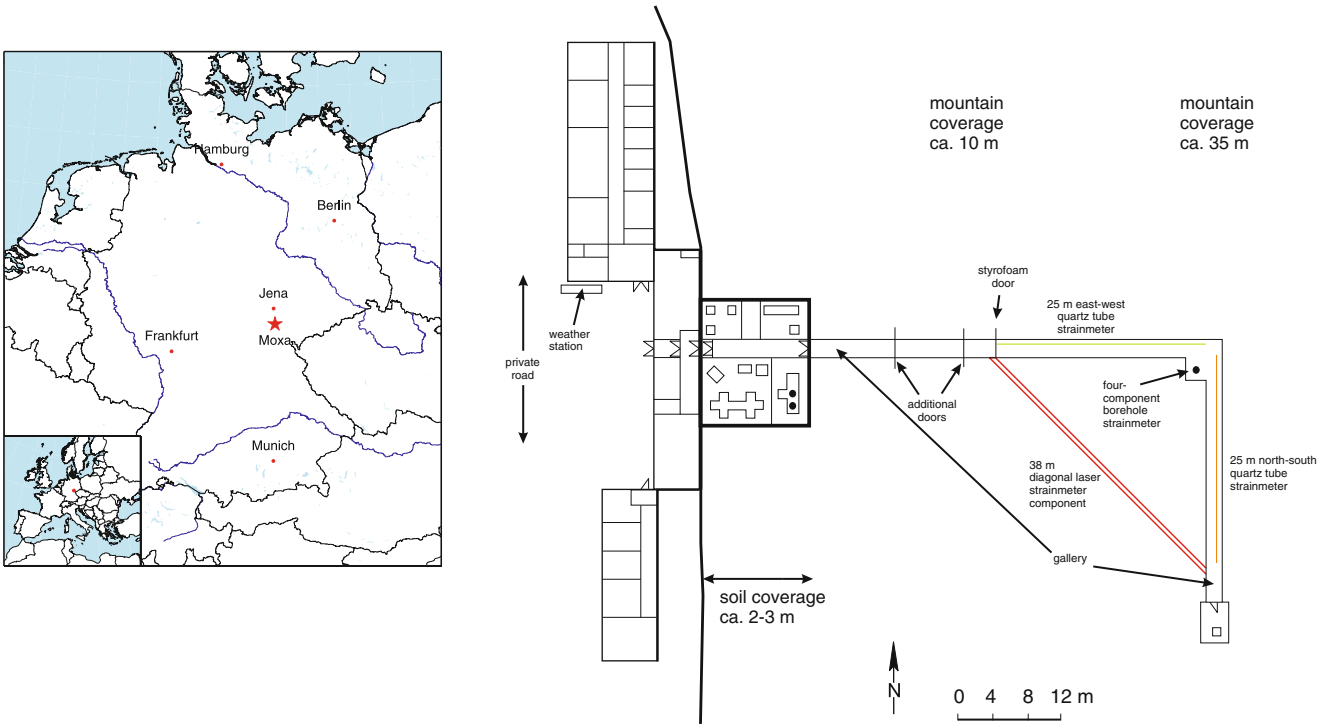

Fig. 1 Map indicating the location of the Geodynamic Observatory Moxa in Germany and Europe; plan view of the observatory building showing the gallery with the installed strainmeters (please note the North arrow; after Jahr et al. 2001)

well as a spring gravimeter (for details see Jahr et al. 2001). Additionally, outside the observatory and in the surrounding area a large number of sensors record environmental parameters like air pressure, temperature, wind, or soil moisture.

All four strainmeters are installed inside the gallery. The ~26 m long quartz tube strainmeters and the ~38 m long laser strainmeter are connected to the ground by steel pillars whereas the borehole instrument is installed at about 10 m depth and the borehole filled up with concrete. The quartz tube strainmeters are oriented in east-west and north-south direction, respectively, along the two arms of the gallery. The laser instrument connects the far ends of the quartz tube strainmeters through a horizontal borehole, and the borehole strainmeter is installed at the gallery elbow (Fig. 1). Unfortunately, of originally three components (with azimuth angles of 90°, 210° and 330°, respectively), only the one with 210° azimuth angle (approximately perpendicular to that of the laser instrument) is still working. The other two components were destroyed by stroke of lightning.

Distance changes along the two quartz tube strainmeters are measured by inductive sensors. The laser strainmeter uses the principle of the Michelson interferometer (Michelson 1881, 1882). To minimize the influence of temperature and air pressure changes on the interference fringes due to the dependence of the refractivity index of air on these values (Edlén 1966; Ciddor 1996, 2002), the horizontal borehole is sealed at both ends with a special glass. The borehole strainmeter was developed by H. Ishii (cf. Ishii et al. 1997, 2002; Ishii 2002) and manufactured and installed by MACOME Corp., Japan; the deformation signal is mechanically amplified by a factor of about 40 (Jentzsch et al. 2006) and then picked up by a magnetic sensor.

All data are sampled every 10 s. In addition, inside the gallery several sensors measure variations in temperature, air pressure or humidity. At the laser strainmeter, another air pressure sensor is installed and five temperature sensors are placed at different points along the laser beam. Outside the observatory building, a meteorologic station records environmental parameters. For some of these parameters an influence on the measurements inside the gallery is already shown (e.g., Gebauer et al. 2010), for others it is assumed.

3 Data Treatment and Results

Data of all four strainmeters and for the same period of time have been analysed. The time-series (Fig. 2) started on August 23, 2008 and ended on December 17, 2009, thus spanning 482 days. We chose that period because it is almost free of data gaps and large disturbances of any origin. Former results can be found in Jahr et al. (2006). As the two quartz tube instruments, which were originally invented as strain-seismometers, have azimuth angles of 0°

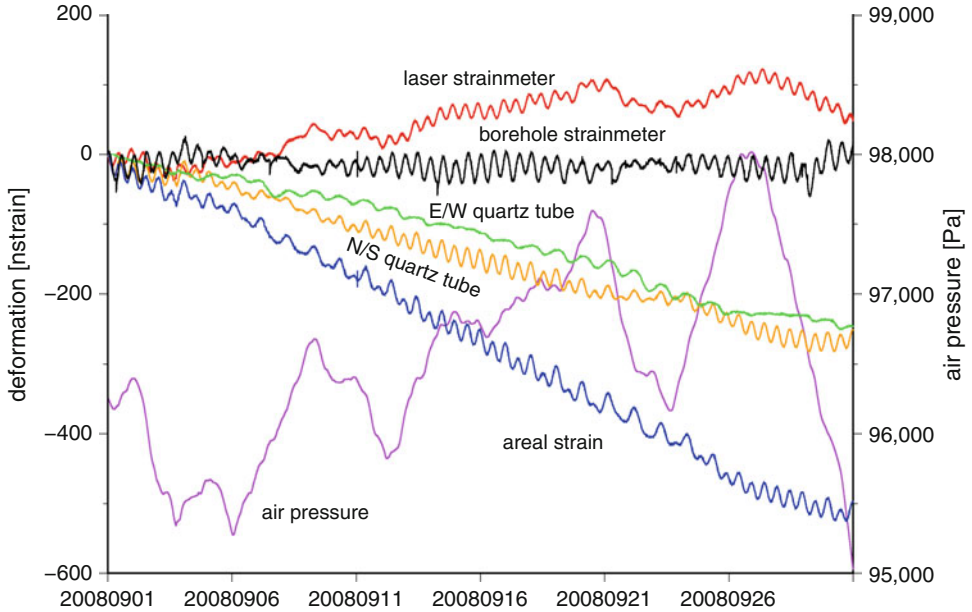

Fig. 2 Sample of all five time-series which were used for analysis; the sample spans the month of September 2008. Air pressure is also given for comparison

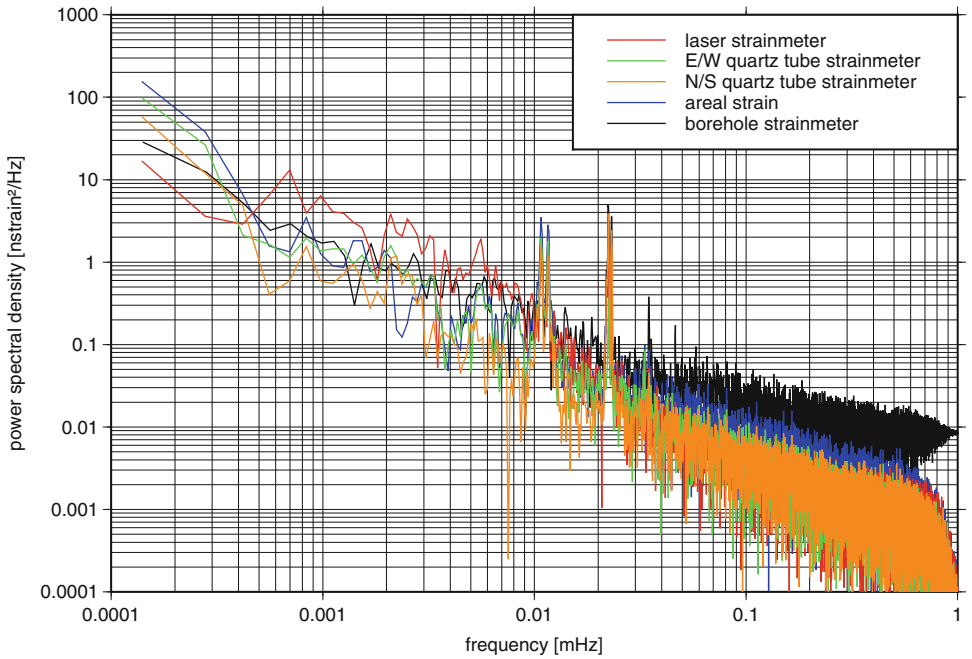

Fig. 3 Power spectra of the five time-series. For higher frequencies (above 0.02 mHz) the noise level of the laser and the two quartz tube strainmeters is almost the same, whereas the areal strain shows a slightly higher noise level. The noise level of the borehole strainmeter is up to one order of magnitude higher than of the three other instruments

and 90°, respectively, for each time step the values of these two can be summed up to get the areal strain in the horizontal plane. The time-series of areal strain has therefore also been investigated.

Figure 3 shows power spectra of all five time-series. The noise level for frequencies above the semi-diurnal tides is two to three orders of magnitude below the tidal signal and also the diurnal tides are contained significantly.

All data have been corrected for steps and smaller gaps were interpolated. Afterwards a numerical filter was used to generate time-series with hourly values from the 10 s data. The conversion from the measured distance changes to strain is obtained by dividing the data by the according base length of the particular instrument. As (except for the laser strainmeter where air pressure has by far the highest influence on the instrument by changing the refractivity index of air) the Earth tides are the main signal in the strain data, the time-series were then analysed with the software package ETERNA (Wenzel 1996). This software calculates the amplitude factors (i.e. observed amplitude divided by theoretical amplitude) and phase shifts for different tidal waves; the theoretical amplitude factor is 1.0. It also allows for the determination of regression coefficients between the

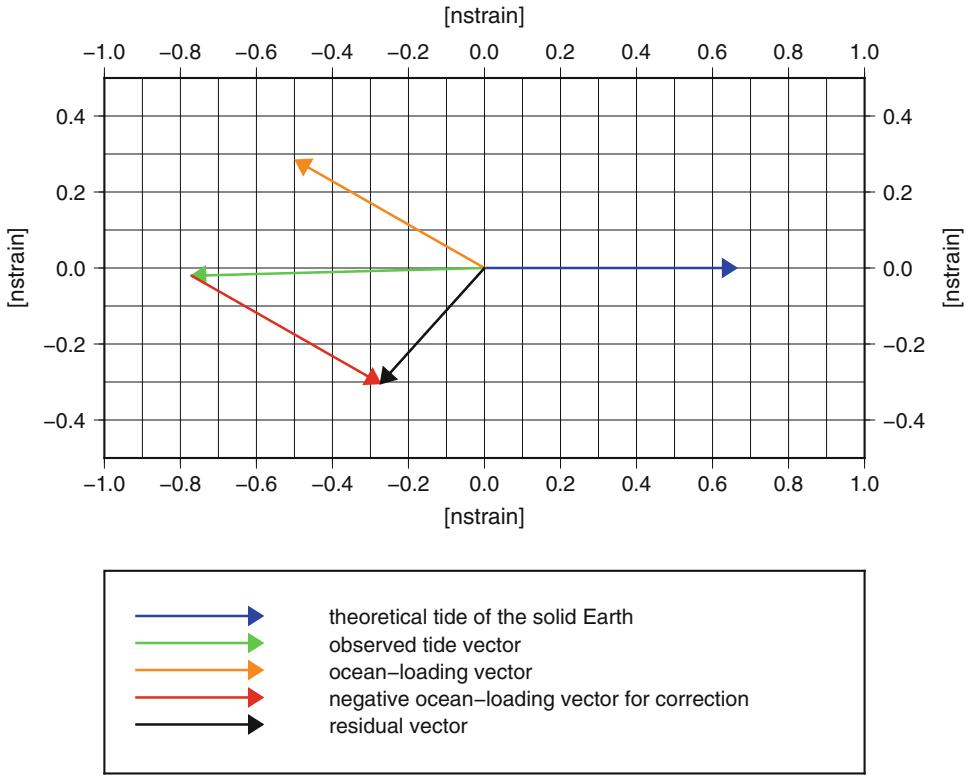

Fig. 4 Example of tidal phasors for tidal wave M2 and the E/W quartz tube strainmeter illustrating the correction of the observed tide for the ocean loading effect

deformation time-series and other time-series of environmental parameters. This method has been used to eliminate the high influence of air-pressure variations on the time-series of the laser strainmeter.

The ocean tides of the North Atlantic and especially of the North Sea have high amplitudes of several meters. Therefore ocean loading effects have to be considered in the surrounding regions. We have calculated the ocean loading for the main diurnal and semi-diurnal tidal waves, using the software GOTIC2 (Matsumoto et al. 2001) with the ocean tide model NAO.99b (Matsumoto et al. 2000). We have then subtracted the loading effect from the observed tides. Figure 4 shows an example for tidal wave M2 and the E/W quartz tube strainmeter.

The results of the tidal analysis for the main diurnal and semi-diurnal waves can be seen in Fig. 5, comparing the observed tides to the residual tides after subtraction of the ocean loading effect. In the diurnal band all five time-series show small phase shifts: the E/W quartz tube strainmeter has a small negative phase value, the laser strainmeter a slightly more negative one. The N/S quartz tube shows only minor positive phase shifts whereas in the data of the borehole strainmeter the phase shifts are the largest ones. The areal strain shows no significant phase shifts at all. The amplitude factors of the five time-series vary between 0.38 and 0.68; the highest values were found for the N/S quartz tube and the borehole instrument. This difference may be due to the fact that these two instruments are farthest away from the gallery entrance and have the highest mountain coverage; therefore their data are less disturbed by changes of the environmental conditions outside the gallery. Such disturbances may also enlarge the amplitude factors depending on their phase shifts. An evaluation of amplitudes and phases of the disturbing effects could be made by means of numerical modelling; this has not been done yet. The ocean loading effect is small for all three tidal waves and for all five time-series.

In the semi-diurnal frequency band the E/W quartz tube strainmeter shows phase shift variations at high values while the other four time-series have only phase shifts up to 20°. The strong variations in the results for the E/W quartz tube instrument are due to the geographic latitude of the Geodynamic Observatory Moxa which approximately coincides with a line of nodes for the semi-diurnal tidal modes, thus having very small absolute values for the amplitudes in the E/W strain component; thus the different modes cannot be separated significantly. The laser strainmeter shows small positive phases, the N/S quartz tube instrument and the areal strain have phase shifts of zero or slightly below; the borehole strainmeter shows always negative phase shifts in the semi-diurnal band. The amplitude factors are larger than in the diurnal band; they range from 0.66 to 1.42, with one exception of 0.60 for the E/W quartz tube strainmeter and tidal wave K2. The largest values were found in the borehole strainmeter data; this instrument shows amplitude factors above 1 for all three main semi-diurnal modes. The amplitude factors for laser strainmeter, N/S quartz tube

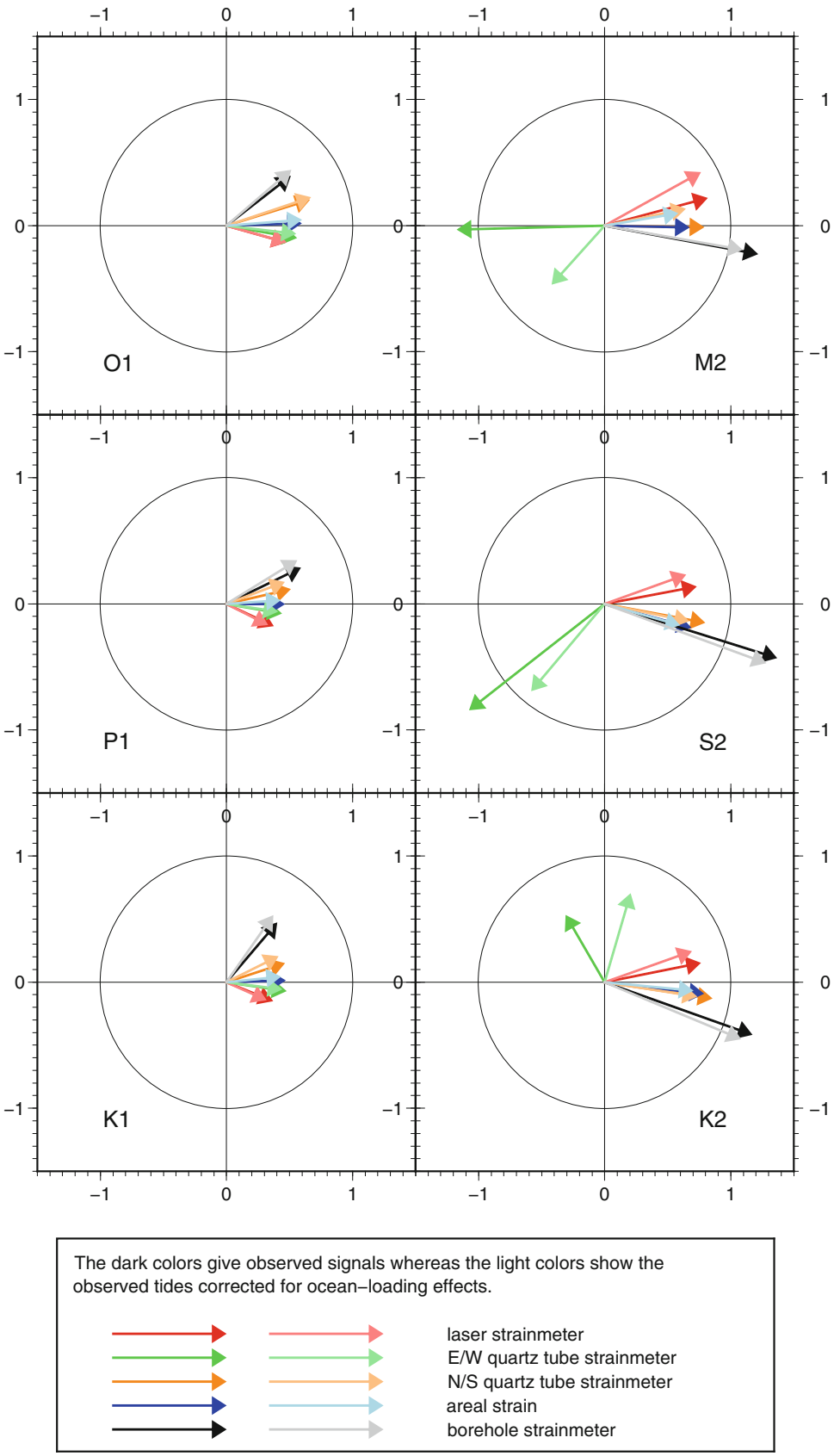

Fig. 5 Phase diagrams of the main diurnal and semi-diurnal tidal waves, showing the observed tides as well as the residual tides after correcting for the ocean loading effects. The arrow length gives the amplitude factor (observed/residual amplitude divided by theoretical amplitude). The deviation from horizontal positive axis denotes the phase shift (phase-lead: counter-clockwise deviation)

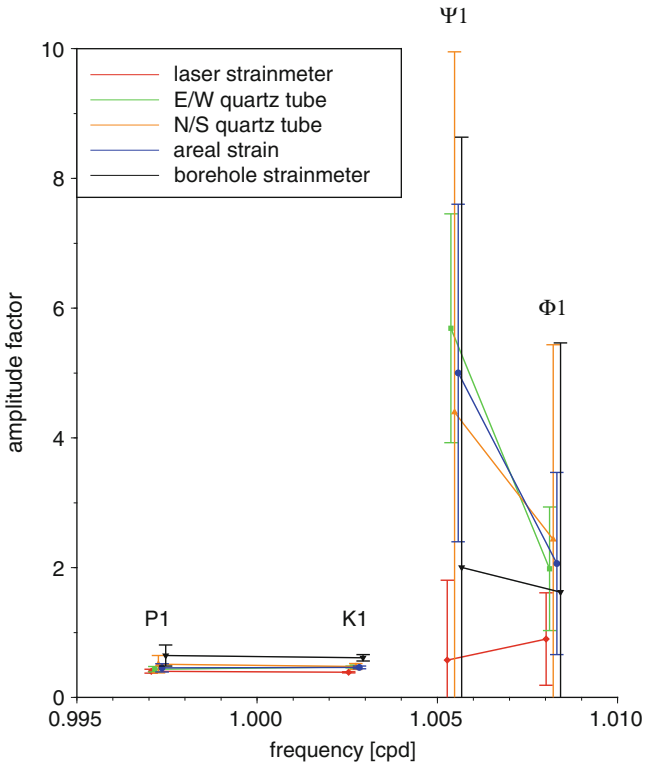

Fig. 6 Amplitude factors of the tidal waves around the resonance frequency of the Nearly Diurnal Free Wobble of the Earth (NDFW). The error bars are 2σ

instrument and areal strain vary between 0.66 and 0.85. For the areal strain they are always smaller than for the N/S quartz tube strainmeter whereas for the laser strainmeter they do not show such a consistent behaviour. Taking into account the ocean loading, especially the E/W quartz tube strainmeter data show strong changes. The phase shifts are clearly reduced. The amplitude factors become smaller in particular for M2 and S2. Regarding the other time-series, only the laser strainmeter shows considerable changes with slightly increased phase shifts compared to the original data.

Another result which can be achieved from the tidal analyses is the Nearly Diurnal Free Wobble (NDFW) resonance of the Earth's core. This resonance effect is the reaction of the core to the diurnal tidal forcing by which it is excited (a good overview on the NDFW can be found in Zürn 1997). Figure 6 shows the amplitude factors of four tidal waves with frequencies around the resonance frequency for all five time-series. The resonance frequency has been calculated for different Earth models (e.g. Wahr 1981) with results around 1.0048 cpd (cycles per solar day). The amplitude factors should show asymptotic behaviour towards the resonance frequency with a trend towards minus infinity for the modes below and towards plus infinity for the modes above the resonance frequency. As the figure shows not all time-series are affected by the NDFW resonance. Below the resonance frequency all five time-series have similar amplitude factors for the two modes P1 and K1, with a slightly negative trend. Asymptotic characteristics of the data are not obvious due to the large separation from the resonance frequency compared with the two modes Ψ_1 and Φ_1 above the resonance frequency. For these two modes, the E/W quartz tube strainmeter, the areal strain and, with larger errors, also the N/S quartz tube instrument show asymptotic running-in from infinity. For the borehole strainmeter, which has by far the largest errors, as well as for the laser strainmeter no significant asymptotic behaviour is visible.

4 Discussion and Conclusions

The analysis of the five time-series for the Earth tides gives, in general, compatible results. The only exception can be seen in the semi-diurnal tidal waves of the E/W quartz tube strainmeter. It can be well explained by the geographic location of the Geodynamic Observatory Moxa which nearly equals a line of nodes for the E/W component of strain. Therefore the measured amplitudes of the semi-diurnal tidal waves are too small to produce good results during tidal analysis. In the diurnal band the phase shifts of the time-series differ slightly more than in the semi-diurnal band (with the exception of the E/W quartz tube component). Amplitude factors are in the same order of magnitude for each tidal wave of the diurnal band. In the semi-diurnal band, the borehole strainmeter shows amplitude factors between 1.5 and 2 times larger than the N/S quartz tube and the laser strainmeters as well as the areal strain. The E/W quartz tube instrument shows totally different behaviour (cf. discussion above).

As the data from strainmeters normally show very high noise rates, the NDFW resonance can not be found often in such time-series. Mainly such results were obtained using strain data from observation sites with much larger mountain coverage like the Black Forrest Observatory (BFO) in southwest Germany (e.g. Polzer et al. 1996) or the Esashi Earth Tides station (Sato 1991). For both stations a resonance frequency of about 1.005 cpd was found. Taking this into account, the detection of the NDFW resonance in the strain data from the Geodynamic Observatory Moxa is a great success. Also the spectra (Fig. 3) show the good data quality; therefore the resonance can be considered proven. Altogether this confirms former results showing the low noise level of Moxa with data from the superconducting gravimeter (Rosat et al. 2003).

Recently two new laser strainmeters similar to the one already working have been installed. They connect the same fix points as the two quartz tube instruments. This assembly will enable direct comparison between the different measurement systems and therefore help to improve data quality and

detect smaller signals, which has not been possible with the old instruments.

Acknowledgements The laser strainmeter has been developed in cooperation with SIOS Messtechnik company in Ilmenau/Germany. We thank the staff at SIOS, especially Dr. W. Pöschel and Dr. D. Dontsov, for their effort to steadily improve the laser strainmeter. Our thanks go also to W. Kühnel and M. Meininger, technicians at the Geodynamic Observatory Moxa, for their excellent maintenance of all instruments.

This article is based on the Diploma thesis of the first author.

We thank three anonymous reviewers for their comments, which helped to improve the paper.

References

Ciddor PE (1996) Refractive index of air: new equations for the visible and near infrared. Appl Opt 35(9):1566–1573. doi:10.1364/AO.35.001566

Ciddor PE (2002) Refractive index of air: 3. The roles of CO2, H2O, and refractive virials. Appl Opt 41(12):2292–2298. doi:10.1364/AO.41.002292

Edlén B (1966) The refractive index of air. Metrologia 2(2):71–80. doi:10.1088/0026-1394/2/2/002

Gebauer A, Steffen H, Kroner C, Jahr T (2010) Finite element modelling of atmosphere loading effects on strain, tilt and displacement at multi-sensor stations. Geophys J Int 181(3):1593–1612. doi:10.1111/j.1365-246X.2010.04549.x

Ishii H (2002) Environmental effects on strain observation, their applications for geophysical study and necessity of deep borehole observation for noiselessly high quality. Bull d'Inf Marées Terr 137:10907–10908

Ishii H, Yamauchi T, Kusumoto F (1997) Development of high sensitivity borhole strainmeters and application for rock mechanics and earthquake prediction study. In: Sugawara K, Obara Y (eds) Rock stress. Proceedings of the international symposium on rock stress. Balkema, Rotterdam, pp 253–258

Ishii H, Yamauchi T, Matsumoto S, Hirata Y, Nakao S (2002) Development of multi-component borehole instrument for earthquake prediction study, some observed example of precursory and co-seismic phenomena relating to earthquake swarms and application of the instrument for rock mechanics. In: Ogasawara H, Yanagidani T, Ando M (eds) Seismogenic process monitoring. Balkema, Rotterdam, pp 365–377

Jahr T, Jentzsch G, Kroner C (2001) The Geodynamic Observatory Moxa/Germany: instrumentation and purposes. J Geod Soc Jpn 47(1):34–39. doi:10.11366/sokuchi1954.47.34

Jahr T, Kroner C, Lippmann A (2006) Strainmeters at Moxa observatory, Germany. J Geodyn 41(1–3):205–212. doi:10.1016/j.jog.2005.08.017

Jentzsch G, Jahr T, Ishii H (2006) News from the Geodynamic Observatory Moxa: the 4-component borehole strainmeter. Bull d'Inf Marées Terr 141:11245–11252

Matsumoto K, Takanezawa T, Ooe M (2000) Ocean tide models developed by assimilating TOPEX/POSEIDON altimeter data into hydrodynamical model: a global model and a regional model around Japan. J Oceanogr 56(5):567–581. doi:10.1023/A:1011157212596

Matsumoto K, Sato T, Takanezawa T, Ooe M (2001) GOTIC2: A program for computation of oceanic tidal loading effect. J Geod Soc Jpn 47(1):243–248. doi:10.11366/sokuchi1954.47.243

Michelson AA (1881) The relative motion of the Earth and the Luminiferous ether. Am J Sci III 22(128):120–129

Michelson AA (1882) Interference phenomena in a new form of refractometer. Philos Mag V 13(81):236–242. doi:10.1080/14786448208627176

Polzer G, Zürn W, Wenzel HG (1996) NDFW analysis of gravity, strain and tilt data from BFO. Bull d'Inf Marées Terr 125:9514–9545

Rosat S, Hinderer J, Crossley D, Rivera L (2003) The search for the Slichter mode: comparison of noise levels of superconducting gravimeters and investigation of a stacking method. Phys Earth Planet Inter 140(1–3):183–202. doi:10.1016/j.pepi.2003.07.010

Sato T (1991) Fluid core resonance measured by quartz tube extensometers at the Esashi Earth Tides station. In: Kakkuri J (ed) Proceedings of the 11th international symposium on earth tides, Helsinki, 1989. E. Schweizerbart'sche Verlagsbuchhandlung, Stuttgart, pp 573–582

Wahr JM (1981) Body tides on an elliptical, rotating, elastic and oceanless earth. Geophys J R Astron Soc 64(3):677–703. doi:10.1111/j.1365-246X.1981.tb02690.x

Wenzel HG (1996) The nanogal software: Earth tide data processing package ETERNA 3.30. Bull d'Inf Marées Terr 124:9425–9439

Zürn W (1997) The nearly-diurnal free wobble-resonance. Lecture notes in Earth sciences, vol 66. Springer, Berlin, pp 95–109